Krivoshein *et al.*
The Journal of Headache and Pain (2025) 26:112
https://doi.org/10.1186/s10194-025-02041-z

The Journal of Headache and Pain

RESEARCH

Open Access

Differential inhibitory effects of endocannabinoids on neuronal firing of mouse meningeal afferents

Georgii Krivoshein[1*], Adriana Della Pietra[2], Juha Savinainen[3], Arn M. J. M. van den Maagdenberg[1,4] and Rashid Giniatullin[2*]

Abstract

Background Increasing endocannabinoids (endoCBs), anandamide (AEA) and 2-arachidonoylglycerol (2-AG), through inhibition of the degrading hydrolase enzymes, fatty acid amide hydrolase (FAAH) and monoacylglycerol lipase (MAGL), respectively, has been proposed as approach to alleviate migraine pain. Notwithstanding, the impact of AEA and 2-AG on neuronal firing of meningeal afferents, which is relevant to the genesis of migraine pain, remains elusive.

Methods The impact of AEA and 2-AG on meningeal nerve afferent firing was examined through electrophysiological evaluation upon application of 50 mM KCl with or without DMSO, exogenous AEA (10 µM), or 2-AG (10 µM) to separate groups of C57BL/6J mouse hemiskull preparations. At the end of each experiment, capsaicin (1 µM), an agonist of TRPV1 channels, was tested, as a positive control of presumably nociceptive firing. Advanced clustering and spectral analysis on the electrophysiological data allowed differentiating spiking patterns with respect to their temporal and neurochemical profiles. Activity-based protein profiling and liquid chromatography with tandem mass spectrometry was used to assess endogenous FAAH and MAGL activity and determine endogenous levels of AEA and 2-AG in mouse meninges.

Results Local application of endoCBs decreased KCl-induced firing of meningeal nerve afferents, which was most profound for AEA. AEA first produced a short, mild activation in firing, which was followed by a long-lasting reduction. Instead, 2-AG directly led to a short-lasting reduction in firing. Cluster analysis revealed that the transient activation by AEA involved fibers with small-amplitude spikes fired at rates of 1–2 Hz, whereas the persistently suppressed fibers consisted of high-amplitude spikes fired at rates exceeding 10 Hz. Only AEA inhibited subsequent capsaicininduced firing in the afferents long after AEA application, suggesting a broader mode of action for AEA than 2-AG. The more profound inhibitory effects of AEA are consistent with the observed higher activity of FAAH over MAGL and lower level of endogenous AEA than 2-AG in mouse meninges.

Conclusion Our study revealed a stronger anti-nociceptive action of AEA than of 2-AG, as measured by meningeal afferent firing in mouse hemiskulls. This difference can be exploited for relieving migraine pain by primarily increasing the tone of AEA through inhibition of FAAH outside the central nervous system.

Keywords Migraine, Neuronal firing, Anandamide, 2-arachidonoylglycerol, FAAH, MAGL

*Correspondence:
Georgii Krivoshein
g.krivoshein@lumc.nl
Rashid Giniatullin
rashid.giniatullin@uef.fi
Full list of author information is available at the end of the article

Background

Migraine is a debilitating neurovascular brain disorder affecting approximately 15% of the general population and is typically characterized by episodes of unilateral throbbing head pain and other neurological features [1, 2]. Despite the many options to treat patients, which include nonsteroidal anti-inflammatory drugs, serotonin receptor 1B/1D agonists (triptans) and small molecule (gepants) and monoclonal antibodies targeting CGRP(-receptors), sufficient relief is achieved in only half of patients [3]. This highlights the clear need for alternative means of analgesia for patients who do not respond to existing treatments. Migraine pain is thought to be brought about by a persistent activation of the trigeminovascular system (TGVS) that is comprised of nociceptive Aδ- and C-fibers originating from the trigeminal ganglion (TG) and projecting to the meningeal vasculature along with connective tissue [4]. Activation of the TGVS ultimately causes sensitization of higher-order neurons in the central nervous system leading to persistent nociceptive signaling and migraine pain [5], which is modulated by the endocannabinoid (ECB) system [6, 7].

The ECB system entails G-protein coupled receptors (GPCR) cannabinoid 1 (CB1) and cannabinoid 2 (CB2) that are widely expressed in the nervous system [6]. Of them, the CB1 receptor is most abundantly expressed in anatomical migraine pathways. In the presence of CB1 activity, nociceptive signals originating from the peripheral TGVS are blocked and do not reach the central nervous system [8–10] and CB2 receptor activation was shown to counteract acute migraine-like pain in a rat model [11]. The ECB system also contains their endogenous ligands, N-arachidonoylethanolamine (or anandamide) (AEA) and 2-arachidonoylglycerol (2-AG), as well as their main respective degrading hydrolase enzymes fatty acid amide hydrolase (FAAH) and monoacylglycerol lipase (MAGL) [12]. The relevance of the ECB system for migraine pathophysiology already comes from the observation that the level of AEA in cerebrospinal fluid of patients with migraine was found to be reduced [13, 14], which seems in line with the TGVS being activated during a migraine headache.

In this context, ameliorating ECB signaling seems a promising migraine treatment strategy, as it offers 'on-demand' action on nociceptive pathways without the psychotropic effects seen with cannabinoids [15]. A complicating factor when designing a treatment based on modulating the ECS is that the relative endogenous levels of AEA and 2-AG, as well as the endogenous activity of their degrading enzymes FAAH and MAGL, are different for peripheral and central parts of nervous systems implicated in migraine pain. For instance, in TG the activity of MAGL is much higher than that of FAAH, leading to a higher level of AEA, whereas in the cortex the level of 2-AG is much higher (due to higher synthesis even though MAGL and FAAH activity are both high) [16]. Therefore, for an ECB-based treatment to work centrally in the brain, one would need to inhibit both FAAH and MAGL, as was shown feasible in preclinical studies that tested a dual inhibitor [8, 17]. However, given the evidence that migraine pain may have its origin foremost in the peripheral nervous system [18], there is a clear rationale to inhibit FAAH, even though there is ongoing debate regarding the true origin of migraine [19], already because the central nervous system is also involved in migraine. Still, pharmacological inhibition of only FAAH activity significantly attenuated nitroglycerin-induced hyperalgesia [17, 20]. It is worth noting that AEA acts, albeit with lower affinity, also on pro-nociceptive TRPV1 channels in the TGVS [8, 21], hence an effective migraine therapy ideally should also counteract TRPV1 activity. In animal models of migraine, exogenously administered AEA diminished hyperalgesic behavior and was associated with a reduced c-Fos expression in brain areas related to nociceptive signal processing [22].

Overall, there is only limited information regarding the effects of AEA and 2-AG on the peripheral meningeal part of the TGVS, at least in mice, as in rats both endoCBs were shown to reduce meningeal neuronal firing [8]. To gain further insight into the anti-nociceptive mechanisms of endoCBs, we here investigated the effects of exogenously applied AEA and 2-AG on neuronal firing as well as TRPV1 channel activity in peripheral meningeal afferent fibers in mouse hemiskull preparations. Furthermore, we assessed the endogenous levels of AEA and 2-AG, as well as the activity of their degrading enzymes, in mouse meningeal preparations.

Methods

Animals

Isolated mouse hemiskulls and meningeal preparations were obtained from adult female wildtype C57BL/6J mice (N (number of mice) = 26) provided by the Animal House of the University of Eastern Finland (Kuopio, Finland). Mice were bred and housed in individually ventilated cages regulated at 22 °C with appropriate humidity levels and a regular 12-h light/12-h dark cycle. Standard rodent food and water were given ad libitum. During experimental measures, efforts were made to minimize animal suffering in accordance with ARRIVE guidelines.

Reagents

Anandamide (N-arachidonoylethanolamide, AEA), 2-arachidonoylglycerol (2-AG), and capsaicin, were purchased from Tocris Bioscience (Bristol, UK). The dual MAGL/FAAH inhibitor AKU-005 was synthetized at the University of Eastern Finland, (Kuopio, Finland). Stock solutions were prepared in dimethyl sulfoxide (DMSO) and stored at − 20 °C.

Tissue preparation

Mice were sacrificed by CO_2 inhalation followed by cervical dislocation and then decapitated. Subsequent surgical procedures were carried out within 15–20 min at room temperature in artificial cerebrospinal fluid (aCSF), containing (in mM): 120 NaCl, 2.5 KCl, 2 $CaCl_2$, 1 $MgCl_2$, 11 glucose, 24 $NaHPO_4$ and 30 $NaHCO_3$, with 95% O_2/5% CO_2 oxygenation maintained at pH 7.25–7.35. First, the outer side of the skull was cleared of skin and cranial muscles and then divided into two hemiskulls along the sagittal line using a pair of scissors (Fig. 1A). Subsequently, the brain was carefully extracted using a forceps, ensuring the preservation of the trigeminal ganglion (TG). Particular care was taken to maintain the meninges with nerves and vessels attached to the bone tissue inside the hemiskull.

For electrophysiology recordings of spiking activity from meningeal nerve endings, isolated mouse hemiskull preparations (n (number of hemiskulls) = 18 from N = 18 mice) were used and prepared as described previously [23, 24]. Extraction of the brain was done so the recording microelectrode reached the peripheral portion of the meningeal branch (*nervus spinosus*), which branches out of the TG and contains the meningeal nerve endings (Fig. 1B). The isolated hemiskull preparation was then gently fixated to the bottom of the recording chamber and maintained under continuous aCSF perfusion (6–7 mL/min) with a 95% O_2/5% CO_2 oxygenation, and room temperature, throughout the recording period.

For activity-based protein profiling (ABPP) to assess endogenous MAGL and FAAH activity and liquid chromatography coupled with triple quadrupole mass spectrometry (LC–MS/MS) to quantify endogenous AEA and 2-AG levels, meninges (n (number of samples) = 8 from N = 8 mice) were carefully isolated with a forceps, immediately flash-frozen on dry ice, and then stored at − 80 °C until further processing. On the day of the experiment, the meningeal samples were mechanically homogenised in phosphate-buffered saline (PBS) and each sample was evenly divided, with half of the sample used for ABPP and the other half for LC–MS/MS analysis.

Electrophysiology recordings

Inside the isolated hemiskull preparation the distal part of the *nervus spinosus* located between the TG and the intercross with the middle meningeal artery (MMA) was cleaned from surrounding meninges and cut at ~ 1 mm before its entry into the TG using a 30 G needle (Fig. 1B). This distal part of the nerve was inserted into a borosilicate glass microcapillary (GC150 F- 10, Harvard apparatus, Edenbridge, UK) that was filled with aCSF and connected to the recording electrode, while temperature was at room temperature throughout the recording

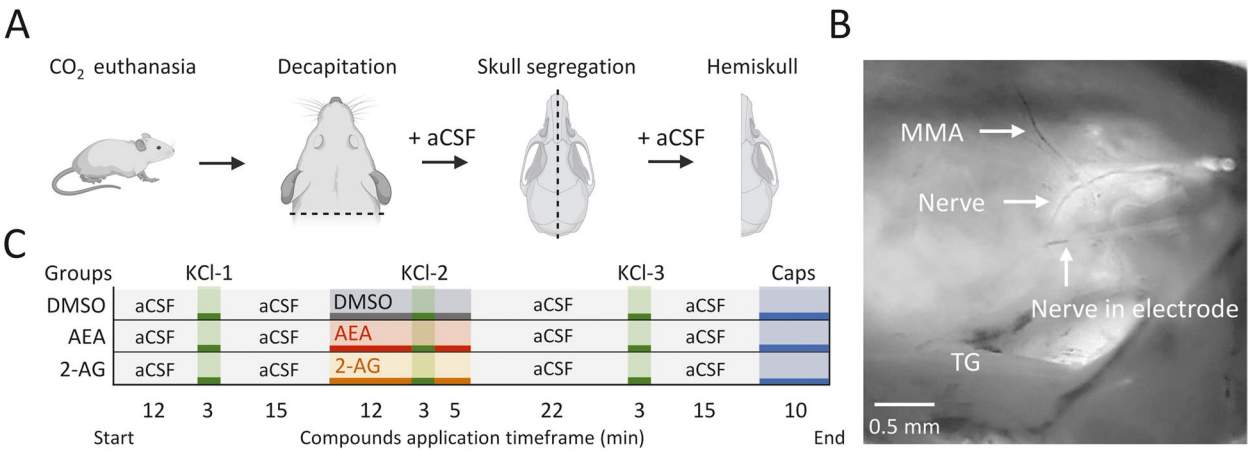

Fig. 1 Experimental approach for meningeal spiking activity recording in a mouse hemiskull preparation. **A** Experimental protocol for mouse hemiskull isolation and preparation. **B** Mouse hemiskull preparation showing meninges with the preserved trigeminal meningeal nerve intersecting with the MMA. The nerve arising from the TG was cut and its peripheral segment was placed into a suction glass electrode for electrophysiological recording. **C** Experimental timeline of applications (for separate DMSO, AEA and 2-AG experimental groups (n = 6 in each group) – so only one compound was applied in a given experiment) as well as the three KCl pulses and a capsaicin application at the end of each experiment. Abbreviations: aCSF, artificial cerebrospinal fluid; TG, trigeminal ganglion; MMA, middle meningeal artery; DMSO, dimethyl sulfoxide; AEA, anandamide; 2-AG, 2-arachidonoylglycerol; Caps, capsaicin. *Panel A was created with BioRender.com*

period. The inserted isolated nerve generated a tight seal by light suction in the glass capillary. Spiking activity from nerve fibers was recorded using a low-noise digital amplifier (ISO 80, World Precision Instruments, Sarasota, FL, USA) with a gain of 10,000X and a bandpass of 300–3,000 Hz. Signals were obtained and digitized at 8-µsec intervals using a NIPCI- 6221 data acquisition board (National Instruments, Austin, TX, USA). Electrical signals were visualised with the WinEDR V3.4.6 software (Strathclyde University, Glasgow, UK) and analysed with MATLAB-based software.

The recordings were carried out for three experimental groups (DMSO, AEA or 2-AG), each consisting of six hemiskulls from different mice. Importantly, only one of the compounds was tested in a particular hemiskull. At the beginning of the experiment, a baseline stabilization recording of spontaneous spiking activity was conducted for 12 min (Fig. 1C). Next, three successive 50 mM KCl applications, so called 'KCl pulses', with compensated osmolarity were applied for 3 min each to induce general nerve excitability. During the second KCl pulse (KCl-2) either DMSO or one of the endoCBs was also applied. The DMSO experiment served as the control, where DMSO was applied following the same timeline and concentration as for the two endoCBs, i.e. AEA (10 µM; the AEA experiment) and 2-AG (10 µM; the 2-AG experiment). All drugs were diluted in aCSF to their final concentration immediately before usage and were applied by fast perfusion (6–7 mL/min) directly to the intersection of the MMA and TG nerve branch (i.e. the receptive field) using cFlow V2. ×8-Channel Switch/Flow Control System Cell MicroControls (Norfolk, UK). EndoCBs were applied 12 min before and remained present during and until 5 min after termination of the second KCl pulse. After this, a washout with aCSF was performed. At the end of the experiment, capsaicin, an agonist of TRPV1 channels, was applied for 10 min (1 µM) to determine neuronal activity from these receptors. Data from the control experiment was compared with data from the two endoCB experiments. Electrophysiological data are presented as raw signal traces, spike frequency time courses (density: 25 spikes/10 s), total spike counts over specific time periods, or as the percentage ratio of spikes before and after compound application.

Cluster and spectral analysis

Cluster analysis was performed as described earlier [25]. To this end, electrophysiological data were filtered at 100–9,000 Hz (IIR, Chebyshev type II filter). Baseline noise variance was calculated for each recording for 20-s long epochs with the minimal variance. The threshold for spike detection was set to five standard deviations (5 SD) and spike amplitudes are presented in arbitrary units (a.u.), which represent peak spike amplitudes normalized to the SD of each record. Spikes were analysed in a time window of 2 ms before and 4 ms after the positive peak of the spike and the following spike parameters were calculated: (1) positive and (2) negative amplitudes; (3) the duration of the positive phase calculated at 10% positive amplitude threshold; and (4) the duration of the negative phase measured at 10% negative amplitude threshold. Analysis of the digitized signal (filtering, detection, calculation of parameters) was performed using the MATLAB software (MathWorks, Natick, MA, USA). Clustering was performed using the KlustaKwik application [26]. In brief, as the preliminary analysis showed an important role of the positive and negative spike amplitudes and durations in the unit identification, positive amplitudes were plotted against the amplitude of the negative phase. The clustering approach allowed division of the total distribution of spikes into 5–29 clusters in each preparation. Cluster spiking activity was normalized to the maximum spiking activity per Hz within each cluster and presented accordingly. Clusters were grouped based on spiking activity changes in response to compound application and presented as a proportion of the total cluster size. For spectral analysis, data were evaluated based on the number of interspike intervals (ISI) per second, considering both whole-nerve activity and individual cluster spike activity. The results are presented as the number of ISIs per unit and the frequency-related activity (in Hz) of each cluster.

Activity-based protein profiling

Homogenised tissue of mouse meninges and TG was subjected to competitive ABPP to investigate the selectivity of inhibitors of endocannabinoid hydrolases FAAH and MAGL, as well as other serine hydrolases present in the tissue. Protein concentrations were assessed using the bicinchoninic acid (BCA) protein assay, as previously described [27]. As described previously [28], the homogenates were pre-treated for 1 h with DMSO, dual MAGL/FAAH inhibitor AKU-005 (100 nM). Pre-treatments were followed by incubation with TAMRA-FP probe (ActivX Fluorophosphonate Probes, Thermo Fisher Scientific Inc., Rockford, IL, USA) (final probe concentration 2 µM) for 1 h at room temperature to label active serine hydrolases. Finally, proteins were loaded onto a SDS-PAGE gel and the proteins were visualized using the ChemiDoc™ MP imaging system (BIO-RAD Laboratories, Hercules, CA, USA) with Cy3 blot application (602/50, Green Epi, Manual Exposure 30–420 s). ImageLab software (BIO-RAD Laboratories) was used for quantification.

Liquid chromatography coupled with triple quadruple mass spectrometry

To measure levels of AEA and 2-AG, LC–MS/MS operated in multiple reaction monitoring scanning mode, as previously validated in tissue homogenates [29]. This method is highly selective and accurate for concentrations within a range of 0.4–70 nM for N-acylethanolamines, such as AEA, and 40–11,000 nM for 2-AG.

Statistical analysis

Statistical analyses were performed using GraphPad Prism (GraphPad Prism Software, San Diego, CA, USA). Data distribution normality was assessed by the Anderson–Darling test. A two-way ANOVA with Tukey's multiple comparison test was used to assess differences between the effects of the three consecutive KCl pulses with and without DMSO and endoCBs application, as well as for comparisons of cluster and spectral results. A one-way ANOVA with Tukey's multiple comparison test was applied to evaluate AEA agonism and the capsaicin effect. Correlation analyses were conducted using Spearman's test. The Wilcoxon signed-rank test was used to compare FAAH vs. MAGL and AEA vs. 2-AG levels. Statistical significance was set at $p < 0.05$, and all values are presented as mean ± standard error of the mean (SEM) or as median with standard deviation (SD) range.

Results

Distinct anti-nociceptive effects of AEA and 2-AG on KCl-induced neuronal firing in meningeal afferents

Possible anti-nociceptive effects of exogenously applied AEA and 2-AG were assessed by investigating their effect on KCl-induced neuronal spiking activity in mouse meningeal afferents. Figure 2A shows example traces of electrophysiological recordings illustrating noticeable differences induced by KCl (50 mM) with DMSO, AEA (10 μM), or 2-AG (10 μM). Figure 2B depicts the variation in spike frequency (presented as density of 25 spikes/10 s) in response to the three KCl pulses with the second KCl pulse (KCl-2) applied under various conditions (i.e. the DMSO, the AEA, or the 2-AG experiment), and capsaicin (1 μM) applied at the end of each experiment. The presence of exogeneous AEA produced a strong inhibitory effect on spiking frequency during the second KCl pulse (as observed by the reduced spiking during KCl-2 compared to KCl-1 that persisted during KCl-3), whereas the inhibitory effect of 2-AG application was notably weaker (as observed by the reduced activity during KCl-2 and recovered activity during KCl-3). During the KCl-2 pulse, the number of spikes in in the presence of AEA reduced to 24.8 ± 6.3% of the number of the KCl-1 pulse (which was set as 100%), while in the presence of 2-AG, this number was reduced to only 45.67 ± 10%. In contrast, in the presence of DMSO, the KCl-2 pulse led to an even less perturbed number of spikes with 88.8 ± 4.6% of the number of the KCl-1 pulse ($p < 0.0001$ vs. AEA; $p = 0.0022$ vs. 2-AG; Fig. 2C).

Changes in spiking activity in response to the KCl-3 pulse, applied after a 22-min aCSF washout, suggest a different neuromodulation for AEA and 2-AG, that is a persistent and steady suppression (i.e. 'tonic inhibitory effect') for AEA and a brief and transient suppression (i.e. 'phasic' inhibitory effect) for 2-AG. This is evidenced by the KCl-3 pulse where the number of spikes in the AEA experiment had decreased further to 11.6 ± 2.8% of the number of the KCl-1 pulse, whereas in the 2-AG experiment the number of spikes had recovered to 70.5 ± 15.5% of the number of the KCl-1 pulse. In the DMSO experiment, the KCl-3 pulse led to a reduction in the number of spikes of 83.5 ± 5.6% of the number of the KCl-1 pulse, so a smaller reduction than for the experiments testing the endoCBs ($p < 0.0001$ vs. AEA; $p < 0.0001$ vs. 2-AG; Fig. 2C). Following the KCl-2 pulse, there is a so-called 'silent time' (no spiking) that was most pronounced in the AEA experiment (9.3 ± 0.7 min) compared to the DMSO (2.7 ± 0.3 min) and the 2-AG (3.2 ± 0.2 min) experiment ($p < 0.0001$ vs. DMSO; $p = 0.0004$ vs. 2-AG; Fig. 2D). Even after the extensive aCSF washout period, the silent time following the KCl-3 pulse remained prolonged at 5.1 ± 0.4 min in the AEA experiment ($p < 0.0001$ vs. DMSO; $p = 0.0004$ vs. 2-AG; Fig. 2D), indicating that the AEA-induced neuronal inhibitory effect persisted over time, consistent with a tonic mode of action. In contrast, in the presence of DMSO and 2-AG, the duration of the silent time remained stable across all three KCl pulses, further highlighting the transient nature of 2-AG's inhibitory effect.

Anti-nociceptive effects of AEA and 2-AG on KCl-induced neuronal firing vary among individual meningeal nerve fibers

To assess whether the anti-nociceptive effects of AEA and 2-AG on KCl-induced neuronal excitability vary for single nerve fibers or small groups of fibers (clusters), a clustering approach was used [25]. Supplemental Fig. 1 A-C shows examples of multiple-spike clusters from KCl-1, KCl-2 and KCl-3 pulses in the DMSO, AEA and 2-AG experiments, whereby each dot represents one spike and different colors indicate different spike clusters. The cluster analysis reveals that in the presence of endoCBs the number of spikes in the various clusters for the KCl-2 pulse is reduced compared to the number of the KCl-1 pulse. However, in contrast to when either DMSO or 2-AG is present, in the presence of AEA, the KCl-2 pulse did hardly activate clusters that consisted of spikes with a relatively large positive or negative amplitude

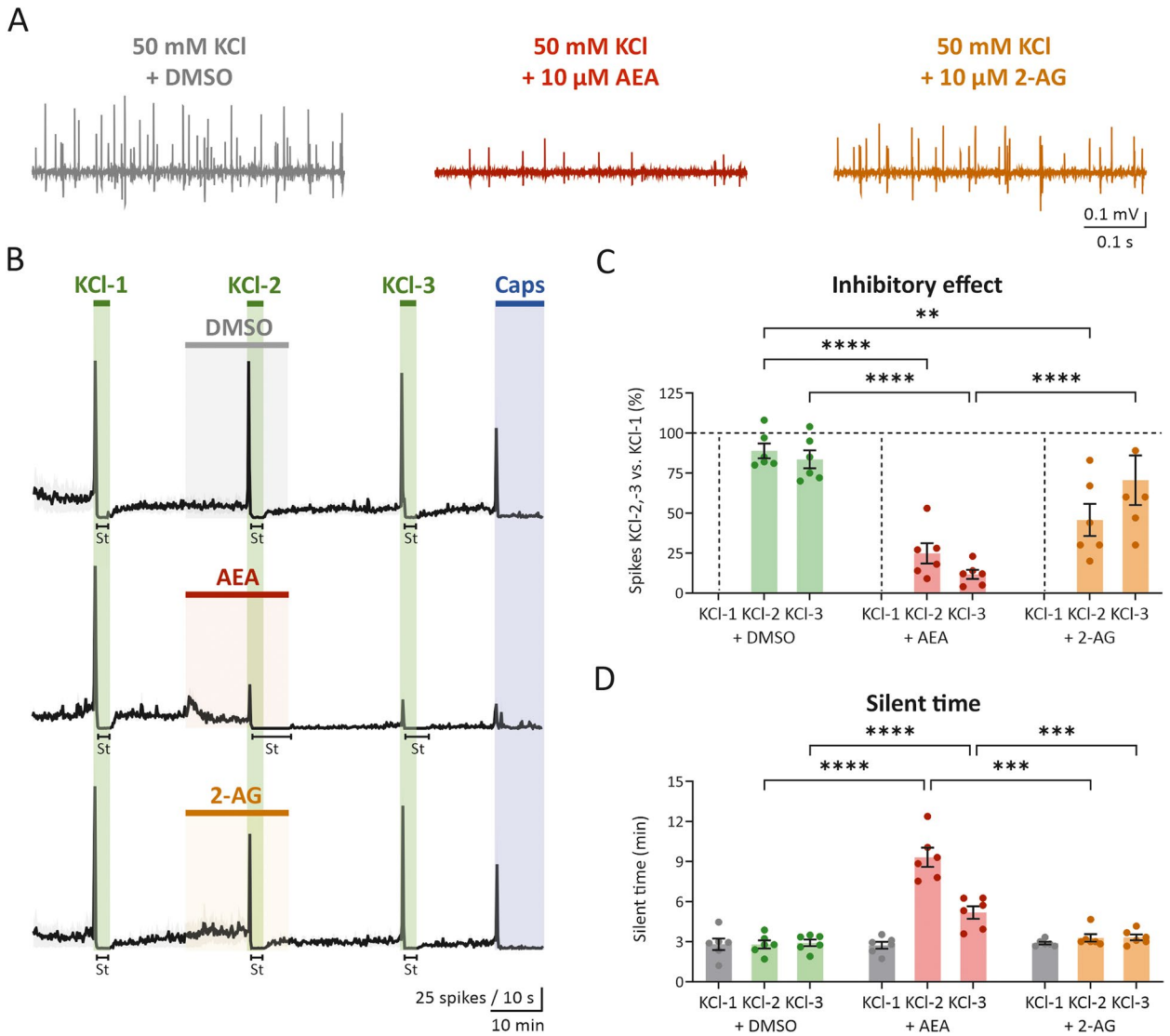

Fig. 2 Changes of KCl-induced meningeal spiking activity within AEA and 2-AG applications. **A** Representative traces of spiking activity recorded from the peripheral part of the trigeminal meningeal nerve during the second KCl (KCl-2) (50 mM) pulse when also DMSO (control), AEA (10 µM) or 2-AG (10 µM), depending on the experiment, were present. **B** Time course of spike frequency (25-s bin size) in response to the three 3-min KCl applications for the DMSO, AEA and 2-AG experiments. At the end of the experiment capsaicin (1 µM) was applied for 10 min. The silent time (St) following a KCl pulse is indicated. **C** AEA resulted in a reduction of KCl-2- and KCl-3-induced spiking activity. In contrast, 2-AG led to a reduction in spiking activity only during the KCl-2 pulse. **D** AEA, but not 2-AG, resulted in a prolonged silent time after the KCl-2 and KCl-3 pulses. Two-way ANOVA was corrected for multiple comparisons using Tukey method (C, D); * $p \leq 0.05$; *** $p \leq 0.001$; **** $p \leq 0.0001$. Abbreviations: DMSO, dimethyl sulfoxide; AEA, anandamide; 2-AG, 2-arachidonoylglycerol; Caps, capsaicin; St, silent time

(Supplemental Fig. 1A-C). To further characterize the neurochemical response across the different clusters, the clusters were classified into four groups based on their spiking activity profile (Fig. 3A-C): (1) *persistently activated*, i.e. spiking activity is increased following both the KCl-2 and the KCl-3 pulse relative to the KCl-1 pulse; (2) *transiently activated*, i.e. spiking activity is increased following the KCl-2 pulse but decreased following the KCl-3 pulse both relative to the KCl-1 pulse; (3) *transiently suppressed*, i.e. spiking activity is decreased following the KCl-2 pulse but recovered following the KCl-3 pulse both relative to the KCl-1 pulse; (4) *persistently suppressed*, i.e. spiking activity is decreased following both the KCl-2 and KCl-3 pulses compared to the KCl-1 pulse. Spiking activity remained consistent for transiently activated fibers across all conditions, while for persistently activated fibers only across the DMSO and 2-AG conditions. In the presence of AEA, transiently and persistently suppressed

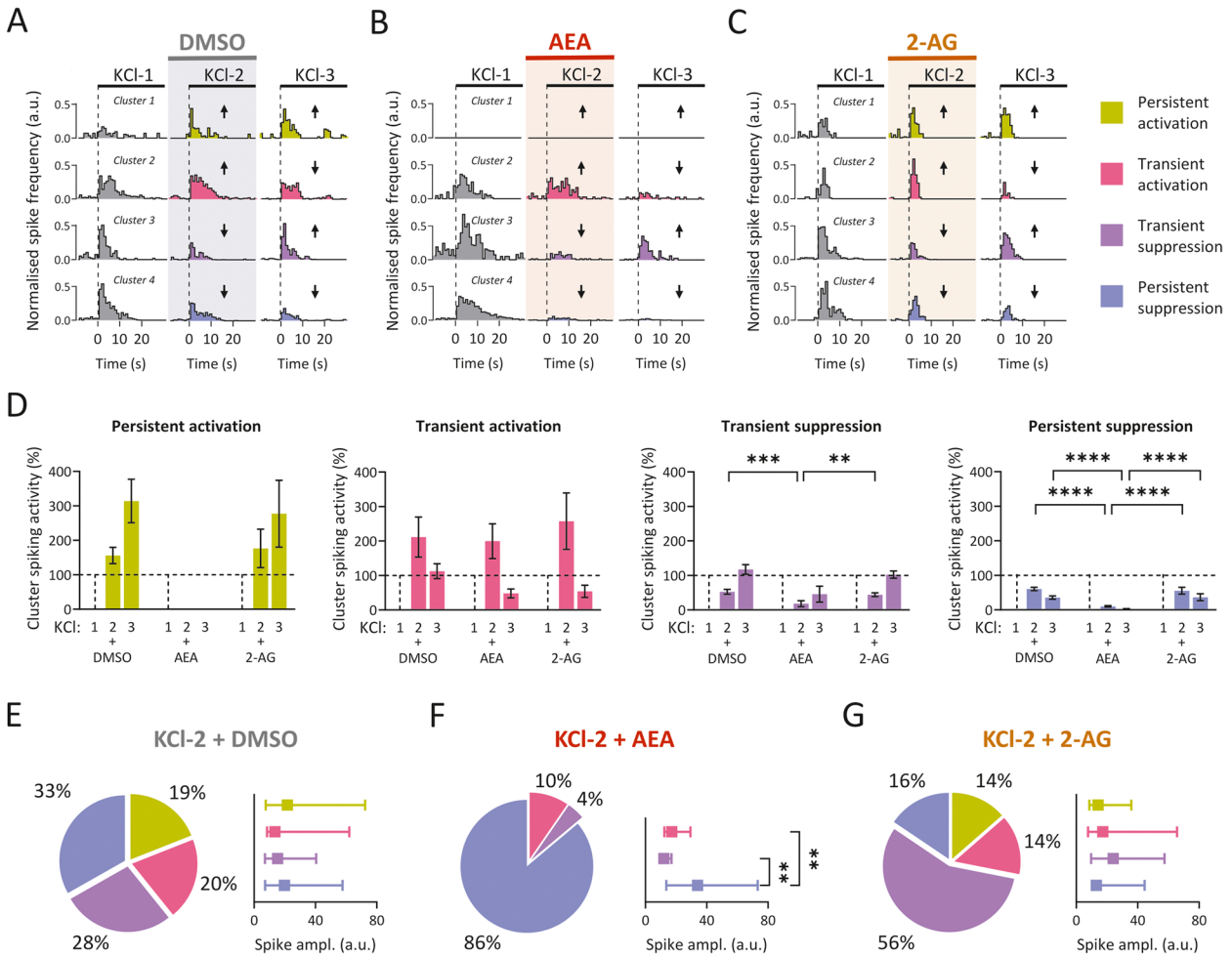

Fig. 3 Cluster analysis of KCl-induced meningeal spiking activity. **A-C** Clustering into four spiking activity groups is based on the respective spiking profiles during the KCl-2 and KCl-3 pulses, relative to the KCl-1 pulse (set as 100%): persistently activated (yellow), transiently activated (pink), transiently suppressed (purple), and persistently suppressed (blue). Spiking activity is normalized to the maximum number of spikes within the KCl pulses independently for each cluster. **D** Comparison of spiking activity profiles among the four spiking activity groups across the various conditions (i.e. 30-s KCl-1, 30-s KCl-2 and 30-s KCl-3 for the DMSO, AEA and 2-AG experiments). **E–G** Pie charts representing the average percentage distribution of clusters among the four spiking activity groups under the various conditions. Next to each pie chart, median spike amplitude with its spread is shown for each spiking activity group. Notably, clusters classified as persistently inhibited accounted for 86% of the population during the KCl-2 pulse in the presence of AEA, exhibiting significantly lower spike amplitudes. In contrast, during the KCl-2 pulse in the presence of 2-AG, the proportion of transiently suppressed clusters doubled compared to when DMSO was present. Two-way ANOVA was corrected for multiple comparisons using Tukey method (D); * $p \leq 0.05$; *** $p \leq 0.001$; **** $p \leq 0.0001$. Abbreviations: DMSO, dimethyl sulfoxide; AEA, anandamide; 2-AG, 2-arachidonoylglycerol; Ampl, amplitude; a.u., arbitrary unit. See also Supplemental Fig. 1

fibers exhibited reduced spiking activity (Fig. 3D). Notably, in the presence of AEA, 86% of clusters were persistently suppressed (Fig. 3F). Persistently activated fibers were entirely absent, while the number of transiently activated fibers was reduced by half (10% vs. 20% in DMSO), and transiently suppressed fibers were seven times fewer (4%) compared to when DMSO was present (28%), highlighting the tonic inhibitory effect of AEA (Fig. 3E-F). In contrast, in the presence of 2-AG, the number of transiently suppressed fibers doubled (56%) compared to when DMSO was present (28%), while the proportion of persistently suppressed fibers was the lowest (16%) across three conditions, emphasizing phasic effect of 2-AG (Fig. 3G). Taken together, cluster analysis revealed that in the presence of AEA, KCl-induced neuronal excitability in peripheral mouse meningeal afferents was suppressed due to the absence of fibers that were capable of being persistently activated, and most importantly due to an increased proportion of fibers that were transiently or persistently suppressed and exhibited a pronounced reduction in large-amplitude spiking activity.

AEA and 2-AG possess variable effects on temporal dynamics of KCl-induced neuronal firing in mouse meningeal afferents

Next, the temporal dynamics of spike activity from meningeal afferents was examined following KCl pulses in the DMSO, AEA, and 2-AG experiments. Spectral analysis showed that the KCl pulses induced spiking activity with very brief interspike intervals (ISI; 0.01–0.1 s), which did not differ for the KCl-1 pulse (Fig. 4A). However, application of AEA prior to the second KCl pulse, reduced KCl-2-induced neuronal firing for the shortest ISI ranges compared to DMSO ($p < 0.0001$ for 0.01–0.02 s; $p = 0.0038$ for 0.04 s; Fig. 4B). Similarly, application of 2-AG reduced KCl-2-induced firing within the same ISI range, though to a lesser extent than seen with AEA ($p = 0.0030$ for 0.01 s; $p = 0.0322$ for 0.02 s; Fig. 4B). Notably, following the extensive washout period after the KCl-2 pulse, the temporal dynamics of KCl-3-induced spiking activity after 2-AG application fully recovered to that when DMSO was present (Fig. 4C). In contrast, in the presence of AEA, the suppression of spiking activity persisted (and even intensified) compared to when DMSO was present ($p < 0.0001$ for 0.01–0.05 s; Fig. 4C), further emphasizing AEA's tonic inhibitory effect. Additionally, following application of AEA prior to the second KCl pulse, clusters with low-spike frequencies (1–2 Hz) showed increased activity during both the KCl-2 ($p = 0.0054$ vs. DMSO; $p = 0.0015$ vs. 2-AG; Supplemental Fig. 2B) and the KCl-3 applications ($p = 0.0175$ vs. DMSO; $p = 0.0006$ vs. 2-AG; Supplemental Fig. 2C). In contrast, in the AEA experiment spiking activity in the range of 3–4 Hz was reduced ($p = 0.0130$ vs. DMSO; Supplemental Fig. 2B), and firing at frequencies above 10 Hz was absent. In this regard, the observed increase in low-frequency firing and reduction in high-frequency firing by AEA may block the temporal summation of nociceptive signals in the periphery, thus potentially preventing nociceptive traffic reaching higher pain centres in the brain.

Distinct effects of AEA and 2-AG on baseline and TRPV1-mediated spiking activity in mouse meningeal afferents

In addition to the abovementioned strong inhibitory effect, AEA also has a small excitatory effect, as shown by the transient increase of spikes during the first 2 min of drug application ($p = 0.03$ vs. the preceding 2 min and $p = 0.01$ vs. the following 2 min; Fig. 5A-B). The number of spikes was increased to 227.7 ± 46.5% (relative to the

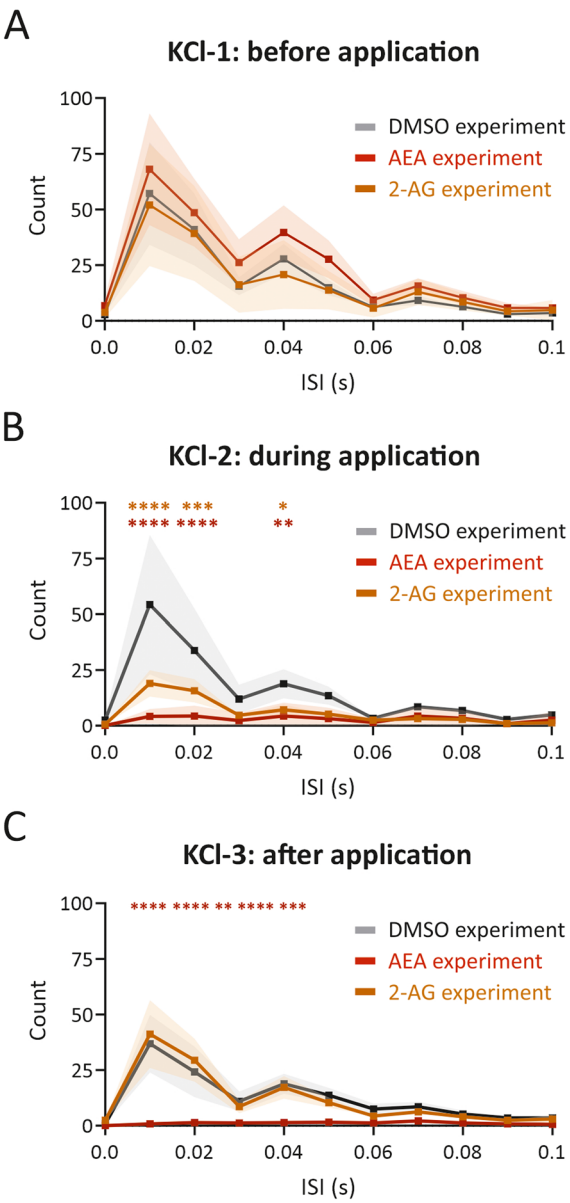

Fig. 4 Spectral analysis of KCl-induced meningeal spiking activity. **A-C** Spectrograms displaying the average interspike intervals (ISI) across the various conditions separated for the three KCl pulses (KCl-1, KCl-2 and KCl-3). **A** ISI during the 30-s KCl-1 pulse before application of DMSO, AEA, or 2-AG. **B** ISI during the 30-s KCl-2 pulse in the presence of DMSO, AEA, or 2-AG. **C** ISI during the 30-s KCl-3 pulse after application of DMSO, AEA, or 2-AG. Two-way ANOVA was corrected for multiple comparisons using Tukey method (**B**, **C**); * $p \leq 0.05$; *** $p \leq 0.001$; **** $p \leq 0.0001$. Abbreviations: DMSO, dimethyl sulfoxide; AEA, anandamide; 2-AG, 2-arachidonoylglycerol; ISI, interspike interval. See also Supplemental Fig. 2

2 min preceding baseline activity) compared to the same timeline of the DMSO (78.7 ± 14.4%; $p = 0.01$; Fig. 5C) and 2-AG (103.8 ± 22.10%; $p = 0.03$; Fig. 5C) experiments. Notably, the clusters that exhibited higher spiking during this 2-min period (32 clusters in total) were also the most active during the subsequent KCl-2 pulse ($r = 0.67$; Fig. 5D), while the silent time for these clusters tended to be shorter ($r = -0.63$; Fig. 5E). Additionally, to explore the possible interaction of AEA agonism with a subsequent TRPV1 channel activation, the spiking activity induced by capsaicin (1 µM) was analysed. The ratio between the 30 s of capsaicin spiking activity and the 30 s of preceding baseline activity was used for comparison across the three experiments. No difference was observed for this ratio when DMSO (1378 ± 271.2%) or 2-AG (1159 ± 330.3%) had been applied. However, when AEA had been applied the ratio was only 427.6 ± 109.7% ($p = 0.04$ vs. DMSO; Fig. 5F). Cluster analysis, used to differentiate clusters that were active during AEA agonism and/or the capsaicin peak (Supplemental Fig. 3), revealed that 62% of the clusters were active under both conditions (Fig. 5G), while only 13% were exclusively activated by capsaicin. The percentage of capsaicin-specific clusters was much higher when DMSO (68%) or 2-AG (74%) had been applied, while clusters that were active in both conditions compiled less than 31% (Fig. 5G).

Endogenous low level of AEA, and not 2-AG, in meninges can explain the neuronal firing patterns seen in mouse meningeal afferents

To analyse the ECB system components in the meninges of female C57BL/6J mice, the in vitro basal activity of the main hydrolyzing enzymes of endoCBs, FAAH and MAGL, was investigated using ABPP (Fig. 6A). The basal activity of FAAH (DMSO pre-application; Fig. 6A) was considerably higher (1.8 ± 0.4 a.u.; Fig. 6B) than that of MAGL (with DMSO pre-application; 0.6 ± 0.1 a.u.; $p = 0.04$; Fig. 6A-B). FAAH and MAGL activities were inhibited by dual FAAH/MAGL inhibitor AKU- 005 (Fig. 6A), as evidenced by the reduced intensity of the respective bands on the gel. The level of AEA (0.006 ± 0.004 pM/ng) was notably lower than the level of 2-AG (0.8 ± 0.2 pM/ng; $p = 0.007$; Fig. 6C), in line with findings of their enzymatic activities. The higher activity FAAH seems to explain the low, almost absent level of endogenous AEA in mouse meninges, and thereby the increased effect on neuronal firing upon exogeneous AEA application. Consequently, the low MAGL activity may explain the higher level of endogenous 2-AG and the less pronounced effect on neuronal firing upon exogeneous 2-AG application. Hence, in particular, increasing the level of endogenous AEA via FAAH inhibition should be the more preferred target for migraine therapeutic intervention of the peripheral part of the nervous system; also because of the longer lasting effect of AEA and inhibiting effect on TRPV1 channels as seen in the experiments.

Discussion

We here employed a detailed electrophysiological approach to compare effects of AEA and 2-AG on neuronal firing, assessed by KCl-induced spiking, of mouse meningeal afferents from hemiskull preparations. We show that AEA exerts a stronger and more sustained anti-nociceptive effect than 2-AG. Interestingly, application of AEA initially caused a mild transient increase of spiking activity, which is likely mediated by activation of TRPV1 channels [30], that was followed by a prolonged suppression of spiking, when KCl was administered to induce excitability of meningeal afferents. The inhibition primarily involved fibers that fired with a high amplitude and high frequency. In contrast, 2-AG produced only a transient inhibitory effect without a preference for certain fibers. Notably, the pronounced anti-nociceptive action of AEA correlated with a low endogenous level of AEA and higher activity of its hydrolyzing enzyme FAAH in meningeal tissue. Combination of the two consistent physiological parameters (i.e. a low level of AEA and a long-lasting inhibitory effect on meningeal neuronal firing) supports a migraine therapy aimed at inhibiting FAAH activity.

Effects of AEA and 2-AG on neuronal firing in meningeal afferents

Both AEA and 2-AG have been shown to reduce KCl-induced spiking activity in meningeal afferents of rats [8], which formed a solid rationale for designing an molecule capable of inhibiting hydrolyzing enzymes FAAH and MAGL [8]. Notably, the short-duration depolarizing testing with a high concentration of KCl, which broadly activates meningeal afferents, creates an efficient platform for testing specific agents for their effects on the peripheral part of the nervous system. Using this platform, we could confirm the anti-nociceptive effects of both endoCBs in mouse meningeal afferents, with AEA having a more profound effect on neuronal firing than 2-AG. Although both endoCBs interact with the CB1 receptor, which is abundantly expressed throughout the nervous system, since AEA is more potent than 2-AG, AEA seems the more relevant endoCB target for migraine therapy, at least for strategically targeting relevant peripheral meningeal nociception. The relevance of AEA to migraine pathophysiology also comes from observations that AEA is capable of inhibiting migraine-relevant neurogenic dural vasodilation as well as CGRP and nitric oxide-induced dural vessel dilation in the rat TGVS [31].

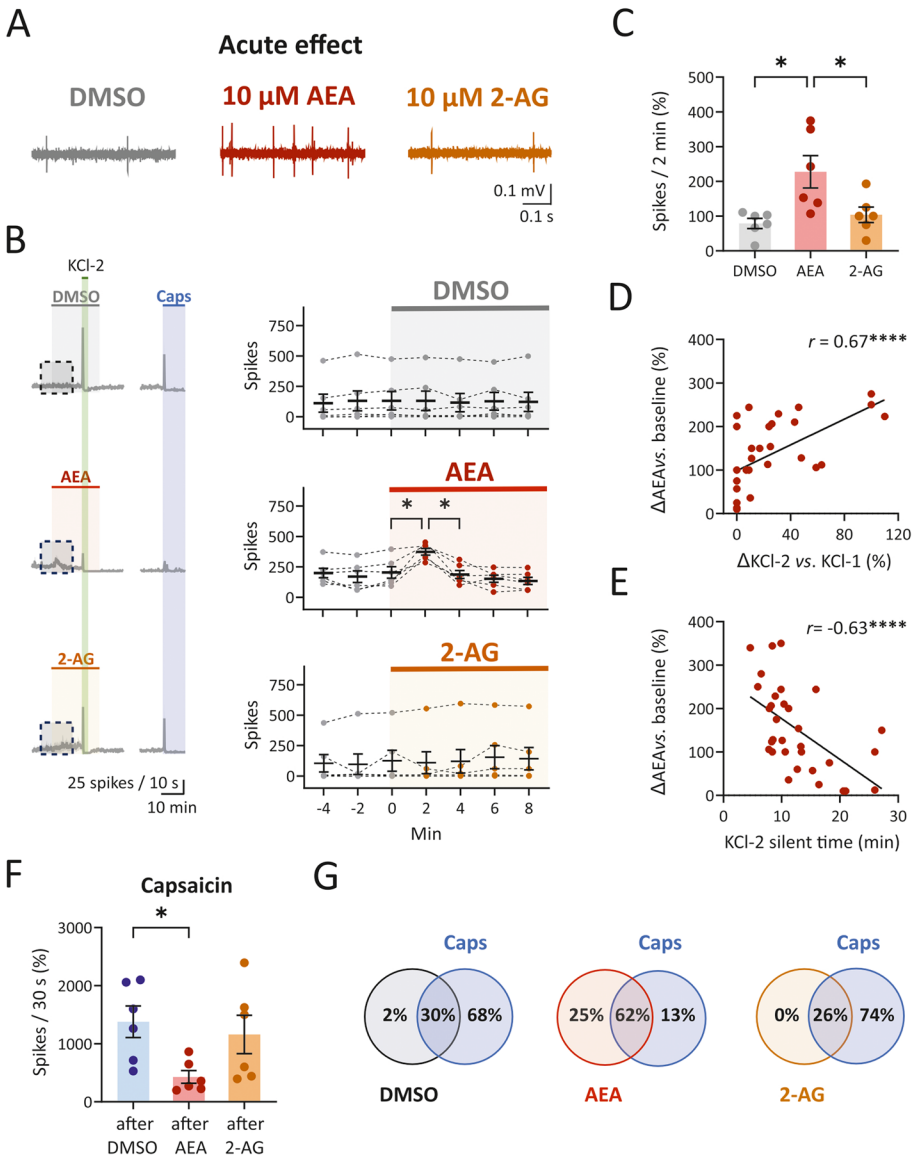

Fig. 5 Effects of exogenous AEA on meningeal baseline and TRPV1 channel spiking activity. **A** Representative traces of spiking activity recorded from the peripheral part of the trigeminal meningeal nerve during the first 2 min after DMSO, AEA (10 µM), or 2-AG (10 µM) application, depending on the experiment. **B** Time course of spike frequency (25-s bin size) with zoomed-in panels (2-min bin size) highlighting the increase in spike numbers during the first 2 min after AEA application. **C** Application of AEA led to a transient increase in spiking activity during the first 2 min, whereas spike frequency was stable when DMSO and 2-AG were applied. **D** Correlation between spiking activity ratios after AEA application (calculated as the ratio of spike frequency during the first 2 min of AEA application and the preceding 2-min baseline) and during the KCl-2 pulse in the presence of AEA (expressed as the ratio of KCl-2 and KCl-1). **E** Correlation between spiking activity ratios during AEA application (as defined above) and the duration of the 'silent time' following the KCl-2 pulse when AEA was present. **F** Application of AEA led to a decreased spiking activity when capsaicin (1 µM) was applied, in comparison to when DMSO had been applied. **G** Overlapping pie charts representing the average percentage distribution of clusters among the three spiking activity groups: activated only during DMSO or AEA or 2-AG; activated during DMSO or AEA or 2-AG and during capsaicin; activated only during capsaicin. One-way ANOVA was corrected for multiple comparisons using Tukey method (**C**, **F**), Spearman's test (**D**, **E**); * $p \leq 0.05$; *** $p \leq 0.001$; **** $p \leq 0.0001$. Abbreviations: DMSO, dimethyl sulfoxide; AEA, anandamide; 2-AG, 2-arachidonoylglycerol; Caps, capsaicin. See also Supplemental Fig. 3

The combined evidence suggests that boosting endoCBs levels, particularly through FAAH inhibition to increase endogenous AEA, seems of high importance in the peripheral nervous system [32].

AEA and 2-AG act on different types of nociceptive fibers

Our advanced cluster analysis revealed that AEA induced the following effects. (1) AEA primarily acted on meningeal fibers that fired with a large amplitude and high

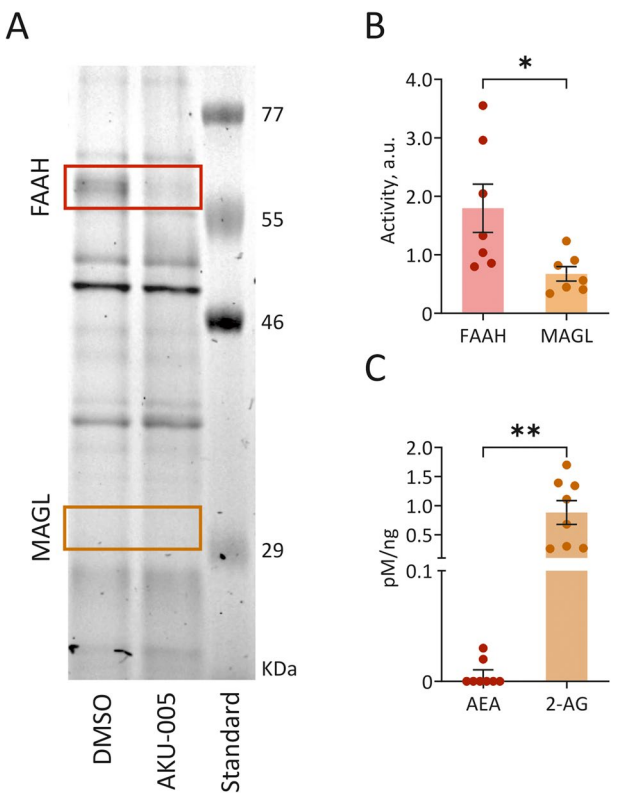

Fig. 6 FAAH activity surpasses MAGL, aligning with lower AEA levels compared to 2-AG in mouse meninges. **A** Mouse meninges were pre-incubated for 1 h with DMSO (vehicle) or dual MAGL/FAAH inhibitor, AKU-005 (100 nM), followed by labelling with the fluorescent probe TAMRA-FP. FAAH and MAGL were identified by inhibition patterns and their expected molecular weights. **B** Basal MAGL and FAAH activities in mouse meninges. FAAH activity was found to be higher than that of MAGL after DMSO treatment. (**C**) LC–MS/MS data showing AEA and 2-AG levels in naïve mouse meninges. The level of AEA level was found lower than that of 2-AG. Wilcoxon test (B, C); * $p \leq 0.05$; *** $p \leq 0.001$; **** $p \leq 0.0001$. Abbreviations: DMSO, dimethyl sulfoxide; AEA, anandamide; 2-AG, 2-arachidonoylglycerol; FAAH, fatty acid amide hydrolase; MAGL, monoacylglycerol lipase; a.u., arbitrary units

frequency. (2) AEA had little effect on fibers that fired with a small amplitude and low frequency (1–2 Hz) as these remained active. (3) AEA initially led to a mild transient increase in firing of fibers the majority of which were responsive to TRPV1-specific agonist. In contrast, 2-AG had a mild transient suppressing effect on KCl activation with modestly reduced high-frequency spiking activity and no change in low-frequency activity, and notably, the spiking activity was restored soon after washout of 2-AG. This difference suggests that AEA and 2-AG seem to target different fibers in the meningeal preparations. Based on our cluster analysis data alone it is difficult to assess whether the activated clusters related to C- or Aδ-fibers. Still one can only speculate that clusters containing spikes with a larger amplitude and higher frequency, as observed during the first KCl pulse, are characteristic of Aδ fibers [33]. It is noteworthy that AEA failed to reactivate these clusters during the second KCl pulse, unlike DMSO and 2-AG. Instead, clusters with a smaller amplitude and lower frequency, which are characteristics typical of C fibers [33], were active and more prominent. This seems to indicate that AEA has a stronger inhibitory effect on Aδ- than C-fibers. This finding aligns well with observations that AEA more effectively inhibits Aδ-fiber-mediated excitatory transmission [34]. Also, CB1 mRNA is predominantly expressed in large-diameter myelinated fibers, a characteristic of Aδ fibers [35], so AEA may preferentially modulate the activity of larger myelinated fibers, likely through CB1 receptor activation. Thus, we show that the two key endoCBs have their own signature when it comes to meningeal neuronal firing. Notably, AEA exerts a stronger inhibitory effect on high-amplitude spiking with rates exceeding 10 Hz, as these fibers are primarily responsible for transmitting nociceptive signals, with pain intensity correlating to neuronal firing frequency.

TRPV1 channels seem to mediate the initial excitatory effect of AEA

AEA is one of several endogenous cannabinoid receptor agonists of TRPV1 channels. Consistent with this, AEA initially acted in an excitatory mode, which involves TRPV1 channels [36], and then acted in an inhibitory mode that is independent of TRPV1 channels [9, 31]. Also in our hemiskull model with meningeal afferents, the initial mild transient increase in spiking after application of AEA (i.e. its excitatory effect), is likely TRPV1-mediated, as we have previously shown that such increase was abolished when the afferents were pretreated with TRPV1 antagonist capsazepine [8]. Notably, the clusters activated during the excitatory phase remained responsive to a subsequent KCl pulse and displayed a greater ability to return to baseline after the pulse. Fibers in these clusters fire with a small amplitude and low frequency, and given that TRPV1 channels are predominantly expressed on C-fibers [37], the excitatory effect of AEA seems due to activation primarily of C-fibers. Additional evidence for this comes from the fact that capsaicin-induced TRPV1-mediated neuronal firing predominantly involved the same type of clusters.

Conclusion

As shown for rat and human tissue before [8], also in mouse meninges the level of endogenous 2-AG is higher than that of AEA, consistent with view that 2-AG participates in tonic inhibition in this tissue. We demonstrated

that exogenous AEA had a stronger inhibitory effect on meningeal afferent firing than 2-AG, suggesting a more potent anti-nociceptive role for AEA. This differential effect on neuronal firing of the two key endoCBs is in sync with the lower level of AEA compared to that of 2-AG. The latter is also in line with the greater activity of FAAH compared to that of MAGL in the meninges. Conceptually, inhibition of FAAH should increase endogenous AEA concentrations to an analgesic level, which would efficiently reduce neuronal spiking activity, and therefore potentially offer a promising novel approach to alleviate migraine pain peripherally. Thus, given that AEA was the endoCB with the more pronounced effect on inhibiting meningeal afferent activity, a FAAH-selective approach may likely offer adequate therapeutic precision [32], when targeting the peripheral part of the nervous system. Considering the mild transient activation of TRPV1 receptors by AEA, it may be worthwhile to consider combining the mentioned therapeutic strategy with one that contains a TRPV1 inhibitor.

Abbreviations

2-AG	2-Arachidonoylglycerol
ABPP	Activity-based protein profiling
AEA	Anandamide
aCSF	Artificial cerebrospinal fluid
CB1	Cannabinoid receptor type 1
CB2	Cannabinoid receptor type 2
CGRP	Calcitonin gene-related peptide
DMSO	Dimethyl sulfoxide
ECB	Endocannabinoid
endoCB	Endogenous cannabinoid
FAAH	Fatty acid amide hydrolase
GPCR	G-protein coupled receptor
LC–MS/MS	Liquid chromatography coupled with triple quadrupole mass spectrometry
MAGL	Monoacylglycerol lipase
MMA	Middle meningeal artery
PBS	Phosphate-buffered saline
SD	Standard deviation
SEM	Standard error of the mean
TG	Trigeminal ganglion
TGVS	Trigeminovascular system
TRPV1	Transient receptor potential vanilloid 1

Supplementary Information

The online version contains supplementary material available at https://doi.org/10.1186/s10194-025-02041-z.

Supplementary Material 1.

Supplementary Material 2.

Supplementary Material 3.

Supplementary Material 4.

Authors' contributions

RG, JS and AMJMvdM supervised the project. GK and ADP sampled mouse meninges, TGs and hemiskulls. GK conducted the electrophysiological experiments. GK performed the cluster analysis and analysed the electrophysiological data. ADP performed the ABPP and LC–MS/MS and analysed the respective data. GK conceptualised the study and wrote the original draft of the manuscript. GK performed the statistical analyses and made the figures. All authors edited the text of the manuscript.

Funding

This work was supported by 2019 Migraine Research Foundation Impact Award (to RG and JS). ADP was supported by the Doctoral Program in Molecular Medicine (DPMM) of the University of Eastern Finland and by OLVI-säätiö (2021). GK was supported by the Finnish National Agency for Education (EDUFI, 2020) and the Dutch National Epilepsy Foundation (2022–10 to AMJMvdM). The work is linked to the Center for Discoveries in Migraine (CDM), which is a Center of Excellence funded by the Danish National Research foundation (to AMJMvdM).

Data availability

The datasets used and analyzed in the current study are available from the corresponding author on reasonable request.

Declarations

Ethics approval and consent to participate

All experimental procedures performed in this study follow the rules of the European Community Council Directive of September 22, 2010 (2010/63/EEC). The Animal Care and Use Committee of the University of Eastern Finland (licence EKS- 008–2019) approved all experimental protocols.

Consent for publication

All authors reviewed and approved the manuscript.

Competing interests

ADP is on the editorial board of The Journal of Headache and Pain but was not involved in the peer review process of this manuscript.

Author details

[1]Department of Human Genetics, Leiden University Medical Center, Leiden, The Netherlands. [2]A.I. Virtanen Institute for Molecular Sciences, University of Eastern Finland, Kuopio, Finland. [3]School of Pharmacy, Faculty of Health Sciences, University of Eastern Finland, Kuopio, Finland. [4]Department of Neurology, Leiden University Medical Center, Leiden, The Netherlands.

Received: 18 March 2025 Accepted: 17 April 2025
Published online: 12 May 2025

References

1. Headache Classification Committee of the International Headache Society (IHS) The International Classification of Headache Disorders, 3rd edition (2018) Cephalalgia 38(1):1–211. https://doi.org/10.1177/0333102417738202
2. Ferrari MD, Goadsby PJ, Burstein R, Kurth T, Ayata C, Charles A, Ashina M, van den Maagdenberg AMJM, Dodick DW (2022) Migraine Nat Rev Dis Primers 8(1):2. https://doi.org/10.1038/s41572-021-00328-4
3. Hong JB, Lange KS, Overeem LH, Triller P, Raffaelli B, Reuter U (2023) A scoping review and meta-analysis of anti-CGRP monoclonal antibodies: predicting response. Pharmaceuticals 16(7):934. https://doi.org/10.3390/ph16070934
4. Goadsby PJ, Lipton RB, Ferrari MD (2002) Migraine-current understanding and treatment. N Engl J Med 346(4):257–270. https://doi.org/10.1056/NEJMra010917
5. Burstein R, Noseda R, Borsook D (2015) Migraine: multiple processes, complex pathophysiology. J Neurosci 35(17):6619–6629. https://doi.org/10.1523/JNEUROSCI.0373-15.2015
6. Leimuranta P, Khiroug L, Giniatullin R (2018) Emerging role of (Endo) cannabinoids in migraine. Front Pharmacol 9:420. https://doi.org/10.3389/fphar.2018.00420
7. Greco R, Demartini C, Zanaboni AM, Francavilla M, De Icco R, Ahmad L, Tassorelli C (2022) The endocannabinoid system and related lipids as potential targets for the treatment of migraine-related pain. Headache 62(3):227–240. https://doi.org/10.1111/head.14267

8. Della Pietra A, Krivoshein G, Ivanov K, Giniatullina R, Jyrkkänen HK, Leinonen V, Lehtonen M, van den Maagdenberg AMJM, Savinainen J, Giniatullin R (2023) Potent dual MAGL/FAAH inhibitor AKU-005 engages endocannabinoids to diminish meningeal nociception implicated in migraine pain. Journal of Headache and Pain 24(1):38. https://doi.org/10.1186/s10194-023-01568-3
9. Akerman S, Holland PR, Goadsby PJ (2007) Cannabinoid (CB1) receptor activation inhibits trigeminovascular neurons. J Pharmacol Exp Ther 320(1):64–71. https://doi.org/10.1124/jpet.106.106971
10. Clapper JR, Moreno-Sanz G, Russo R, Guijarro A, Vacondio F, Duranti A, Tontini A, Sanchini S, Sciolino NR, Spradley JM, Hohmann AG, Calignano A, Mor M, Tarzia G, Piomelli D (2010) Anandamide suppresses pain initiation through a peripheral endocannabinoid mechanism. Nat Neurosci 13(10):1265–1270. https://doi.org/10.1038/nn.2632
11. Greco R, Mangione AS, Sandrini G, Nappi G, Tassorelli C (2014) Activation of CB2 receptors as a potential therapeutic target for migraine: evaluation in an animal model. J Headache Pain 15(1):14. https://doi.org/10.1186/1129-2377-15-14
12. Battista N, Di Tommaso M, Bari M, Maccarrone M (2012) The endocannabinoid system: an overview. Front Behav Neurosci 6:9. https://doi.org/10.3389/fnbeh.2012.00009
13. Sarchielli P, Pini LA, Coppola F, Rossi C, Baldi A, Mancini ML, Calabresi P (2007) Endocannabinoids in chronic migraine: CSF findings suggest a system failure. Neuropsychopharmacology 32(6):1384–1390. https://doi.org/10.1038/sj.npp.13012468
14. Greco R, Demartini C, Zanaboni AM, Piomelli D, Tassorelli C (2018) Endocannabinoid system and migraine pain: an update. Front Neurosci 12:172. https://doi.org/10.3389/fnins.2018.00172
15. Poudel S, Quinonez J, Choudhari J, Au ZT, Paesani S, Thiess AK, Ruxmohan S, Hosameddin M, Ferrer GF, Michel J (2021) Medical cannabis, headaches, and migraines: a review of the current literature. Cureus 13(8):17407. https://doi.org/10.7759/cureus.17407
16. Della Pietra A, Giniatullin R, Savinainen JR (2021) Distinct activity of endocannabinoid-hydrolyzing enzymes MAGL and FAAH in key regions of peripheral and central nervous system implicated in migraine. Int J Mol Sci 22(3):1204. https://doi.org/10.3390/ijms22031204
17. Greco R, Demartini C, Francavilla M, Zanaboni AM, Tassorelli C (2021) Dual inhibition of FAAH and MAGL Counteracts migraine-like pain and behavior in an animal model of migraine. Cells 10(10):2543. https://doi.org/10.3390/cells10102543
18. Olesen J, Burstein R, Ashina M, Tfelt-Hansen P (2009) Origin of pain in migraine: evidence for peripheral sensitisation. Lancet Neurol 8(7):679–690. https://doi.org/10.1016/S1474-4422(09)70090-0
19. Do TP, Hougaard A, Dussor G, Brennan KC, Amin FM (2023) Migraine attacks are of peripheral origin: the debate goes on. J Headache Pain 24(1):3. https://doi.org/10.1186/s10194-022-01538-1
20. Greco R, Francavilla M, Demartini C, Zanaboni AM, Facchetti S, Palmisani M, Franco V, Tassorelli C (2023) Activity of FAAH-Inhibitor JZP327A in an experimental rat model of migraine. Int J Mol Sci 24(12):10102. https://doi.org/10.3390/ijms241210102
21. Fischer MJ, Messlinger K (2007) Cannabinoid and vanilloid effects of R(+)-methanandamide in the hemisected meningeal preparation. Cephalalgia 27(5):422–428. https://doi.org/10.1111/j.1468-2982.2007.01312.x
22. Greco R, Mangione AS, Sandrini G, Maccarrone M, Nappi G, Tassorelli C (2011) Effects of anandamide in migraine: data from an animal model. J Headache Pain 12(2):177–183. https://doi.org/10.1007/s10194-010-0274-4
23. Krivoshein G, Tolner EA, van den Maagdenberg AMJM, Giniatullin RA (2022) Migraine-relevant sex-dependent activation of mouse meningeal afferents by TRPM3 agonists. J Headache Pain 23(1):4. https://doi.org/10.1186/s10194-021-01383-8
24. Krivoshein G, Bakreen A, van den Maagdenberg AMJM, Malm T, Giniatullin R, Jolkkonen J (2022) Activation of meningeal afferents relevant to trigeminal headache pain after photothrombotic stroke lesion: a pilot study in mice. Int J Mol Sci 23(20):12590. https://doi.org/10.3390/ijms232012590
25. Zakharov A, Vitale C, Kilinc E, Koroleva K, Fayuk D, Shelukhina I, Naumenko N, Skorinkin A, Khazipov R, Giniatullin R (2015) Hunting for origins of migraine pain: cluster analysis of spontaneous and capsaicin-induced firing in meningeal trigeminal nerve fibers. Front Cell Neurosci 9:287. https://doi.org/10.3389/fncel.2015.00287
26. Kadir SN, Goodman DF, Harris KD (2014) High-dimensional cluster analysis with the masked EM algorithm. Neural Comput 26(11):2379–2394. https://doi.org/10.1162/NECO_a_00661
27. Navia-Paldanius D, Patel JZ, López Navarro M, Jakupović H, Goffart S, Pasonen-Seppänen S, Nevalainen TJ, Jääskeläinen T, Laitinen T, Laitinen JT, Savinainen JR (2016) Chemoproteomic, biochemical and pharmacological approaches in the discovery of inhibitors targeting human α/β-hydrolase domain containing 11 (ABHD11). Eur J Pharm Sci 93:253–263. https://doi.org/10.1016/j.ejps.2016.08.031
28. Navia-Paldanius D, Savinainen JR, Laitinen JT (2012) Biochemical and pharmacological characterization of human α/β-hydrolase domain containing 6 (ABHD6) and 12 (ABHD12). J Lipid Res 53(11):2413–2424. https://doi.org/10.1194/jlr.M030411
29. Lehtonen M, Storvik M, Malinen H, Hyytiä P, Lakso M, Auriola S, Wong G, Callaway JC (2011) Determination of endocannabinoids in nematodes and human brain tissue by liquid chromatography electrospray ionization tandem mass spectrometry. J Chromatogr 879(11–12):677–694. https://doi.org/10.1016/j.jchromb.2011.02.004
30. Muller C, Lynch DL, Hurst DP, Reggio PH (2020) A closer look at anandamide interaction with TRPV1. Front Mol Biosci 7:144. https://doi.org/10.3389/fmolb.2020.00144
31. Akerman S, Kaube H, Goadsby PJ (2004) Anandamide is able to inhibit trigeminal neurons using an in vivo model of trigeminovascular-mediated nociception. J Pharmacol Exp Ther 309(1):56–63. https://doi.org/10.1124/jpet.103.059808
32. Greco R, Demartini C, Zanaboni AM, Tumelero E, Reggiani A, Misto A, Piomelli D, Tassorelli C (2020) FAAH inhibition as a preventive treatment for migraine: A pre-clinical study. Neurobiol Dis 134:104624. https://doi.org/10.1016/j.nbd.2019.104624
33. MacIver MB, Tanelian DL (1993) Structural and functional specialization of A delta and C fiber free nerve endings innervating rabbit corneal epithelium. J Neurosci 13(10):4511–4524. https://doi.org/10.1523/JNEUROSCI.13-10-04511.1993
34. Luo C, Kumamoto E, Furue H, Chen J, Yoshimura M (2002) Anandamide inhibits excitatory transmission to rat substantia gelatinosa neurones in a manner different from that of capsaicin. Neurosci Lett 321(1–2):17–20. https://doi.org/10.1016/s0304-3940(01)02471-5
35. Price TJ, Helesic G, Parghi D, Hargreaves KM, Flores CM (2003) The neuronal distribution of cannabinoid receptor type 1 in the trigeminal ganglion of the rat. Neuroscience 120(1):155–162. https://doi.org/10.1016/s0306-4522(03)00333-6
36. Pacher P, Bátkai S, Kunos G (2004) Haemodynamic profile and responsiveness to anandamide of TRPV1 receptor knock-out mice. J Physiol 558(2):647–657. https://doi.org/10.1113/jphysiol.2004.064824
37. Ichikawa H, Sugimoto T (2001) VR1-immunoreactive primary sensory neurons in the rat trigeminal ganglion. Brain Res 890(1):184–188. https://doi.org/10.1016/s0006-8993(00)03253-4

Publisher's Note